© 2017. Published by The Company of Biologists Ltd | Journal of Cell Science (2017) 130, 2579-2590 doi:10.1242/jcs.199729

RESEARCH ARTICLE

Rab7 palmitoylation is required for efficient endosome-to-TGN trafficking

Graziana Modica[1,*], Olga Skorobogata[1,*], Etienne Sauvageau[1], Adriano Vissa[2,3,4], Christopher M. Yip[3,4], Peter K. Kim[2,3], Hugo Wurtele[5,6] and Stephane Lefrancois[1,7,‡]

ABSTRACT

Retromer is a multimeric protein complex that mediates endosome-to-trans-Golgi network (TGN) and endosome-to-plasma membrane trafficking of integral membrane proteins. Dysfunction of this complex has been linked to Alzheimer's disease and Parkinson's disease. The recruitment of retromer to endosomes is regulated by Rab7 (also known as RAB7A) to coordinate endosome-to-TGN trafficking of cargo receptor complexes. Rab7 is also required for the degradation of internalized integral membrane proteins, such as the epidermal growth factor receptor (EGFR). We found that Rab7 is palmitoylated and that this modification is not required for membrane anchoring. Palmitoylated Rab7 colocalizes efficiently with and has a higher propensity to interact with retromer than nonpalmitoylatable Rab7. Rescue of Rab7 knockout cells by expressing wild-type Rab7 restores efficient endosome-to-TGN trafficking, while rescue with nonpalmitoylatable Rab7 does not. Interestingly, Rab7 palmitoylation does not appear to be required for the degradation of EGFR or for its interaction with its effector, Rab-interacting lysosomal protein (RILP). Overall, our results indicate that Rab7 palmitoylation is required for the spatiotemporal recruitment of retromer and efficient endosome-to-TGN trafficking of the lysosomal sorting receptors.

KEY WORDS: Rab7, Retromer, Palmitoylation, Endosomes, Post-translational modifications, Intracellular trafficking

INTRODUCTION

Retromer is an evolutionarily conserved multimeric complex first identified in the yeast *Saccharomyces cerevisiae* as responsible for the retrieval of a vacuolar protein sorting receptor, Vps10p, from the prevacuolar compartment to the trans-Golgi network (TGN) (Seaman et al., 1997, 1998). In yeast, retromer is a pentameric complex composed of a conserved trimer, Vps26p, Vps29p and Vps35p, which is responsible for cargo recognition (referred to as cargo selective complex, CSC), and a dimer of sorting nexins (SNXs), Vps5p and Vps17p (Horazdovsky et al., 1997). Yeast strains deleted of each of the retromer subunits are unable to correctly traffic the lysosomal enzyme carboxypeptidase Y (CPY) to the vacuole and secrete it into the extracellular space (Bonangelino et al., 2002). In humans, the retromer CSC is conserved (Haft et al., 2000), and can associate with a varying combination of SNXs, thereby expanding the range of cargos that can be recognized and trafficked (Cullen, 2008; Gallon and Cullen, 2015). In human cells, retromer is responsible for the retrieval of cargo receptors from the endosome to the TGN (Arighi et al., 2004; Seaman, 2004), and is required for the recycling of transmembrane proteins from the endosomal compartment to the plasma membrane (Burd and Cullen, 2014; Feinstein et al., 2011; Steinberg et al., 2013; Temkin et al., 2011). Increasing evidence has underlined how alterations in retromer expression or mutations in its subunits are associated with several neurodegenerative diseases, including Alzheimer's disease and Parkinson's disease (Follett et al., 2017; Small and Petsko, 2015).

Rab7 (also known as RAB7A) and its yeast homolog Ypt7 are responsible for the recruitment and stabilization of the retromer CSC at the endosome (Balderhaar et al., 2010; Burd and Cullen, 2014; Rojas et al., 2008; Seaman et al., 2009). Deletion of Ypt7 in yeast is associated with CPY secretion (Bonangelino et al., 2002) and cargo receptor accumulation at the endosome (Liu et al., 2012). In human cells, siRNA-mediated downregulation of Rab7 expression is associated with displacement of the CSC from the endosomal membrane to the cytosol, and with secretion of the lysosomal hydrolase cathepsin D (Rojas et al., 2008; Seaman et al., 2009).

In addition to its role in retromer recruitment, Rab7 also regulates endosome/lysosome fusion events via its interaction with Rab-interacting lysosomal protein (RILP) (Cantalupo et al., 2001). RILP, in turn, interacts with the endosomal sorting complex required for transport (ESCRT) system (Progida et al., 2006), mediating the internalization of mono-ubiquitinated transmembrane proteins into multivesicular bodies, leading to their degradation in lysosomes. Furthermore, Rab7 can regulate autophagy by modulating the interaction of lysosomes with autophagosomes (McEwan et al., 2015). How cells regulate the function of Rab7 in these various pathways is not well understood.

A RNAi screen designed to identify integral membrane proteins implicated in endosome-to-TGN trafficking found the palmitoyltransferase (PAT) DHHC5 (Breusegem and Seaman, 2014). PATs are transmembrane proteins characterized by a conserved catalytic domain containing a tetrapeptide of aspartic acid, histidine, histidine and cysteine (DHHC) (Mitchell et al., 2006), and mediate palmitoylation, a reversible attachment of a palmitate chain onto a cysteine of a target protein. Palmitoylation can serve as a reversible membrane anchor, promote localization of proteins to detergent resistant membranes, or modulate protein-protein interaction (Linder and Deschenes, 2007). Furthermore, two yeast PATs, Akr1 and Swf1, were identified in a screen for novel

[1]Centre INRS-Institut Armand-Frappier, Institut National de la Recherche Scientifique, Laval, Québec H7V 1B7, Canada. [2]Program in Cell Biology, The Hospital for Sick Children, Toronto, Ontario M5G 1X8, Canada. [3]Department of Biochemistry, University of Toronto, Toronto M5G 1X8, Canada. [4]Institute of Biomaterials & Biomedical Engineering and Department of Chemical Engineering and Applied Chemistry, University of Toronto, Toronto, Ontario M5S 3E5, Canada. [5]Centre de recherche de l'Hôpital Maisonneuve-Rosemont, Montréal H1T 2M4, Canada. [6]Département de Médecine, Université de Montréal, Montréal, Québec H3C 3J7, Canada. [7]Department of Anatomy and Cell Biology, McGill University, Montreal, Quebec H3A 0C7, Canada.
*These authors contributed equally to this work

‡Author for correspondence (stephane.lefrancois@iaf.inrs.ca)

S.L., 0000-0002-3312-9594

Received 16 November 2016; Accepted 6 June 2017

Journal of Cell Science (2017) 130, 2579-2590 doi:10.1242/jcs.199729

proteins implicated in CPY trafficking, suggesting that these enzymes play a critical role in lysosomal trafficking (Bonangelino et al., 2002).

Here, we show that Rab7 is palmitoylated on two cysteine residues. The nonpalmitoylatable Rab7 mutant, $Rab7_{C83,84S}$, localizes to membranes, suggesting that this modification is not required for membrane anchoring. Lack of Rab7 palmitoylation results in reduced interaction with retromer, leading to less efficient endosome-to-TGN cargo receptor trafficking, which results in the missorting of the lysosomal protein cathepsin D. Interestingly, Rab7 palmitoylation is not required for the degradation of the epidermal growth factor receptor (EGFR) or for the interaction between Rab7 and RILP, suggesting that this post-translational modification on Rab7 is required for its role in endosome-to-TGN trafficking.

RESULTS

Rab7 is palmitoylated on cysteine residues 83 and 84

To determine the role of palmitoylation in modulating endosome-to-TGN trafficking, we first asked if any retromer subunits are palmitoylated as this post-translational modification could act as a reversible membrane anchor for retromer CSC. Owing to the lack of an effective antibody for Vps29, we transfected HEK-293 cells with a FLAG-tagged form of Vps29 [Vps29-$(FLAG)_3$] and performed acyl resin-assisted capture (Acyl-RAC) analysis, a well-characterized method to test for protein palmitoylation (Forrester et al., 2011). None of the retromer CSC subunits were captured in our assay, but we recovered the well-known palmitoylated protein TRAPPC3 (Kummel et al., 2006), suggesting that none of the retromer CSC components are palmitoylated (Fig. 1A).

Rab7 is required to recruit retromer to endosomes (Rojas et al., 2008; Seaman et al., 2009), and was identified in a screen for palmitoylated neuronal proteins (Kang et al., 2008). We hypothesized that Rab7 palmitoylation could affect retromer endosomal recruitment by modulating the activity of this protein. We first tested endogenous Rab7 in HEK-293 cells for palmitoylation using Acyl-RAC and found that this small GTPase is palmitoylated (Fig. 1A), as it was captured in our assay when cells were treated with hydroxylamine (NH_2OH), which cleaves palmitate groups from proteins exposing a free cysteine(s) to interact with the thiopropyl Sepharose beads. Palmitoylation occurs on cysteine residues of proteins and we identified four evolutionarily conserved cysteine residues in Rab7 and Ypt7. The two C-terminal cysteines, 205 and 207 for mammalian Rab7, and

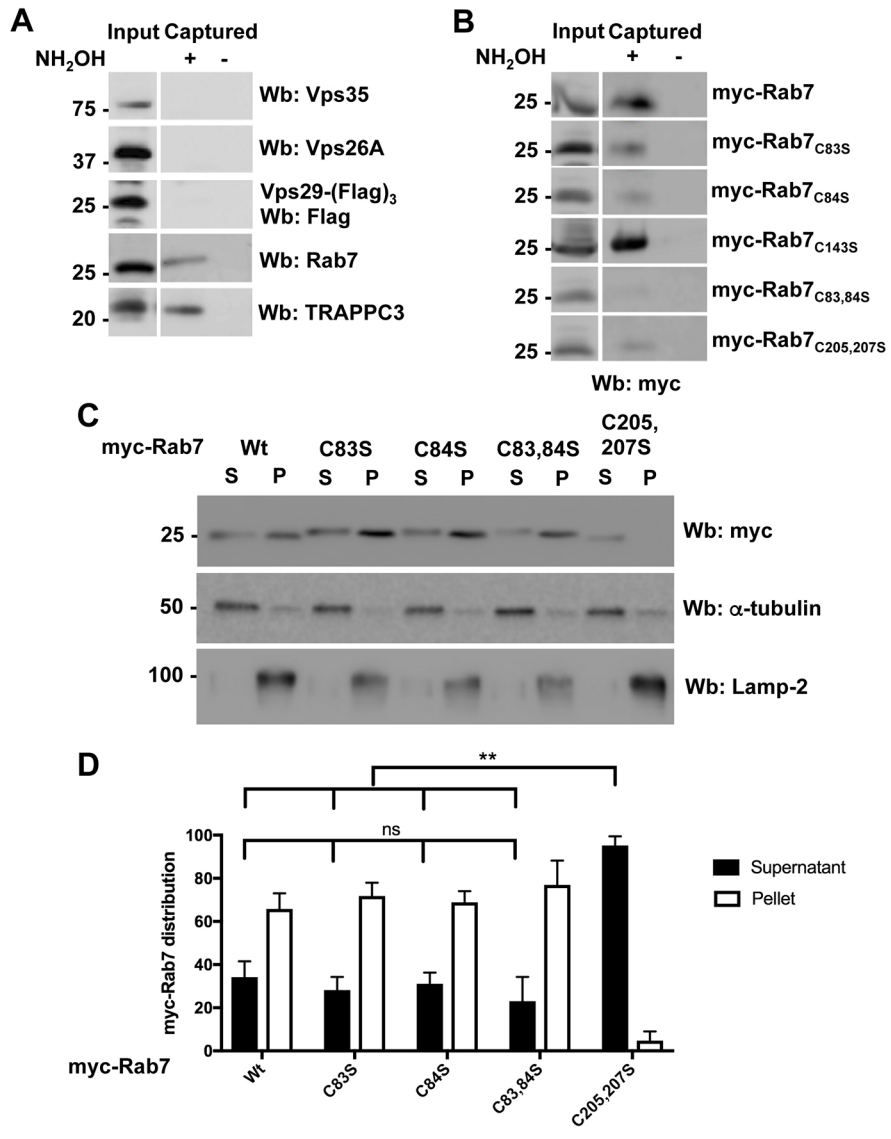

Fig. 1. Rab7 is palmitoylated but this modification is not required for membrane binding. (A) HEK-293 cells were transfected with Vps29-$(FLAG)_3$ and cell lysate was obtained 24 h post-transfection. 30 µl of the whole cell lysate was kept as a loading control (Input) and the remainder was subjected to Acyl-RAC. The eluted samples and Input were loaded onto a 12% acrylamide gel and subjected to WB with anti-Vps35, anti-Vps26A, anti-FLAG, anti-Rab7 and anti-TRAPPC3 antibodies. (B) HEK-293 cells were transfected with Myc-Rab7, Myc-$Rab7_{C83S}$, Myc-$Rab7_{C84S}$, Myc-$Rab7_{C83,84S}$ and Myc-$Rab7_{C205,207S}$. 24 h post-transfection, cell lysates were subjected to Acyl-RAC and WB with anti-Myc antibody was performed. (C) HEK-293 cells were transfected with Myc-Rab7 and the indicated mutants. 24 h post-transfection, membrane separation assays were performed and samples were analyzed via WB with anti-Myc, anti-Lamp-2 (a membrane marker) and anti-α-tubulin (a cytosolic marker) antibodies. S, soluble fraction; P, pellet fraction. (D) Quantification of membrane distribution for the membrane separation experiments in C. Data are mean±s.d. ns, not significant; $^{**}P<0.01$ (one-way ANOVA followed by Tukey's post-hoc test).

Journal of Cell Science (2017) 130, 2579-2590 doi:10.1242/jcs.199729

206 and 208 for yeast Ypt7, are prenylated (Magee and Newman, 1992), a post-translational modification that is required for membrane binding. No post-translational modifications on the other pairs of cysteine residues, 83 and 84 for Rab7, and 84 and 85 for Ypt7, have been described.

To identify the residues targeted by this post-translational modification, we used Myc-tagged Rab7 (Myc-Rab7) and mutated the various cysteines using site-directed mutagenesis. HEK-293 cells were transfected with wild-type Myc-Rab7 and the various mutants, and an Acyl-RAC assay was performed (Fig. 1B). We found that the single cysteine-to-serine mutation of residues 83 or 84 resulted in a decrease in palmitoylation compared to wild-type Rab7, while the double mutant Rab7$_{C83,84S}$ was not recaptured, indicating that it is not palmitoylated (Fig. 1B). Mutation of cysteine 143, not present in Ypt7, did not affect Rab7 palmitoylation (Fig. 1B). Mutation of the two C-terminal cysteines (Rab7$_{C205,207S}$) resulted in a reduction in the palmitoylation level of Rab7 (Fig. 1B). Prenylation of C-terminal cysteines in Rab GTPases serves as a membrane anchor (Chavrier et al., 1991), so the reduction in palmitoylation observed in the prenylation mutants may be caused by the inability of the mutant protein to be membrane associated. Since all known PATs are integral membrane proteins, prenylation and membrane anchoring of Rab7 may be a prerequisite for palmitoylation.

Rab7 palmitoylation is not required for membrane anchoring

To determine how palmitoylation modulates the function of Rab7, we first analyzed the membrane distribution of wild-type and mutant proteins. We transfected HEK-293 cells with wild-type Myc-Rab7 and the various mutants, and performed a membrane separation experiment to determine the amount of Rab7 on membranes. Our separation was successful as the cytosolic protein α-tubulin and the integral membrane protein Lamp-2 were found in the soluble and pellet fraction, respectively (Fig. 1C). As expected, wild-type Rab7 is mostly membrane bound while Rab7$_{C205,207S}$ is localized to the soluble fraction (Fig. 1C). The membrane localization of the Rab7$_{C83S}$, Rab7$_{C84S}$ and the nonpalmitoylatable mutant Rab7$_{C83,84S}$ is comparable to that of wild-type Rab7, suggesting that palmitoylation is not regulating the ability of the protein to bind membranes (Fig. 1C). Statistical analysis of four separate experiments found no significant changes in membrane distribution between Myc-Rab7, Myc-Rab7$_{C83S}$, Myc-Rab7$_{C84S}$ and the nonpalmitoylatable mutant (Myc-Rab7$_{C83,84S}$), while the distribution of the prenylation mutant (Myc-Rab7$_{C205,207S}$) was significantly different from that of the other proteins as it was almost exclusively cytosolic (Fig. 1D).

Palmitoylation can serve as a membrane anchor, or it can serve to localize proteins to specific membrane compartments (Rocks et al., 2005). To test if the palmitoylation of Rab7 modulates its intracellular distribution, we evaluated the localization of wild-type Myc-Rab7, Myc-Rab7$_{C83,84S}$ and Myc-Rab7$_{C205,207S}$ with the early endosomal marker Rab5 (RFP-Rab5) (Fig. 2A-I), as well as their localization with the late endosomal marker RILP (Fig. 2K-S). We found that Myc-Rab7 and Myc-Rab7$_{C83,84S}$ partially colocalized with RFP-Rab5 (R_{wt}=0.2194, $R_{C83,84S}$=0.2554) (Fig. 2J) and more strongly with RILP (R_{wt}=0.4167, $R_{C83,84S}$=0.4832) (Fig. 2T), while Myc-Rab7$_{C205,207S}$ had a negative Pearson's correlation with both RFP-Rab5 ($R_{205,207S}$=−0.02875) (Fig. 2J) and RILP ($R_{205,207S}$=−0.1222) (Fig. 2T) suggesting that this mutant was not found in early or late endosomes, as expected. Overall, our results indicate that palmitoylation is not required for the localization of Rab7 to endosomal membranes.

Rab7 palmitoylation is required for the efficient recruitment of retromer CSC

To test the function of Rab7 palmitoylation, we engineered a Rab7 knockout HEK-293 cell line (Rab7-KO) using CRISPR-Cas9 (Fig. 3A). The absence of endogenous Rab7 allows us to study the function of Rab7 palmitoylation without the background of any residual expression of endogenous wild-type protein (Fig. 3A). To determine whether Rab7 palmitoylation is required for the recruitment of retromer to endosomal membranes, we used a membrane separation experiment. Compared to HEK-293 or HEK-293 cells expressing Myc-Rab7, retromer CSC is displaced to the soluble fraction (cytosol) in Rab7-KO cells (Fig. 3B), as shown by western blotting (WB) for Vps26A and Vps35. This phenotype is rescued by the expression of wild-type Myc-Rab7, but not by Myc-Rab7$_{C205,207S}$ expression. The expression of Myc-Rab7$_{C83,84S}$ did not efficiently restore Vps26A membrane localization (Fig. 3B).

To support our membrane separation assay, we transfected Rab7-KO cells with Myc-Rab7, the nonpalmitoylatable mutant Myc-Rab7$_{C83,84S}$ and the prenylation defective mutant Myc-Rab7$_{C205,207S}$, and examined the intracellular localization of the CSC subunit of retromer via Vps35 immunofluorescence (IF) (Fig. 4). In HEK-293 cells, Vps35 appears in punctate structures characteristic of endosomes (Fig. 4A, arrowheads). In cells not expressing Rab7 (Rab7-KO cells), we observed an almost complete loss of Vps35 endosomal staining (Fig. 4B, asterisks), consistent with previously published results (Rojas et al., 2008; Seaman et al., 2009). Expression of Myc-Rab7 in Rab7-KO cells rescued Vps35 localization to punctate structures (Fig. 4B, arrowheads). Quantification of the fluorescence intensity of Vps35 puncta revealed a significant increase in Rab7-KO cells expressing wild-type Myc-Rab7 compared to nontransfected cells. Interestingly, the expression of Myc-Rab7$_{C83,84S}$ in Rab7-KO cells (Fig. 4C, arrowheads) partially rescued the membrane localization of Vps35, but quantification showed that the increase compared to Rab7-KO cells was not significant. Finally, expression of Myc-Rab7$_{C205,207S}$ failed to rescue Vps35 localization, as expected, since this mutant is not membrane bound (Fig. 4D).

Palmitoylation modulates the interaction between Rab7 and retromer

To better understand how Rab7 palmitoylation is required to recruit retromer, we tested how this post-translational modification affects the interaction between Rab7 and its effectors using bioluminescence resonance energy transfer (BRET), a method that detects molecular proximity in live cells. Wild-type Rab7 and Rab7$_{C83,84S}$ were fused at the N-terminus to the energy donor Renilla luciferase II (RLucII) to obtain RLucII-Rab7 and RLucII-Rab7$_{C83,84S}$, while Vps26A and RILP were fused at the C-terminus with the energy acceptor green fluorescence protein 10 to obtain Vps26A-GFP10 and RILP-GFP10. To ensure that tagging Rab7 with RLucII (RLucII-Rab7) did not affect its membrane localization and function, we performed rescue experiments using membrane separation and IF microscopy to determine if RLucII-Rab7 could restore retromer CSC recruitment in Rab7-KO cells (Fig. S1). Recruitment to membranes was not impaired by the RLucII tag as RLucII-Rab7 was membrane bound (Fig. S1A). Furthermore, RLucII-Rab7 and Myc-Rab7 both rescued retromer CSC membrane recruitment in Rab7-KO cells, as shown by blotting for Vps26A and Vps35 following a membrane separation assay (Fig. S1A). To confirm these results, we expressed Myc-Rab7 or RLucII-Rab7 in Rab7-KO cells immunostained for Vps35 (Fig. S1B) and quantified the fluorescence intensity of Vps35 puncta in

Journal of Cell Science (2017) 130, 2579-2590 doi:10.1242/jcs.199729

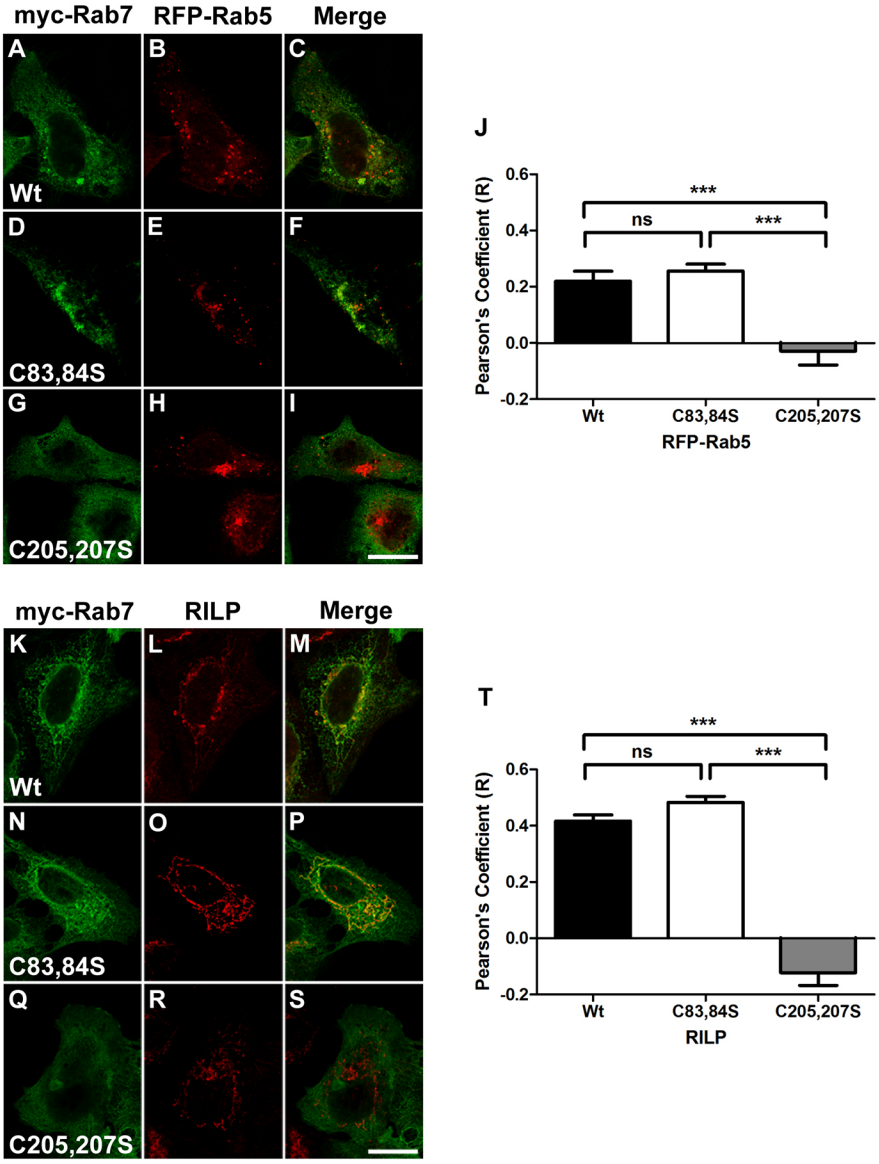

Fig. 2. Palmitoylation is not required to localize Rab7 to late endosomes. (A-I) U2OS cells coexpressing Myc-Rab7 (A,C), Myc-Rab7$_{C83,84S}$ (D,F) or Myc-Rab7$_{C205,207S}$ (G,I) and RFP-Rab5 were immunostained with anti-Myc antibody. Representative images are shown. Scale bar: 10 µm. (J) Pearson's correlation coefficient of Myc-Rab7 (black bar), Myc-Rab7$_{C83,84S}$ (white bar) or Myc-Rab7$_{C205,207S}$ (gray bar) with RFP-Rab5 was calculated from 16, 13 and 16 cells, respectively. (K-S) U2OS cells expressing Myc-Rab7 (K,M), Myc-Rab7$_{C83,84S}$ (N,P) or Myc-Rab7$_{C205,207S}$ (Q,S) were immunostained with anti-Myc and anti-RILP antibodies. Representative images are shown. Scale bar: 10 µm. (T) Pearson's correlation coefficient of Myc-Rab7 (black bar), Myc-Rab7$_{C83,84S}$ (white bar) or Myc-Rab7$_{C205,207S}$ (gray bar) with RILP was calculated from 27, 19 and 23 cells, respectively. ns, not significant; ***P<0.001 (one way ANOVA with Tukey's post hoc test).

Rab7-KO cells (Fig. S1C, black bar), Rab7-KO cells expressing Myc-Rab7 (Fig. S1C, white bar) and Rab7-KO cells expressing RLucII-Rab7 (Fig. S1C, gray bar). Both Myc-Rab7 and RLucII-Rab7 were able to recruit retromer CSC to membranes as statistical analysis of the fluorescence intensity of Vps35 puncta showed a significant increase in both Myc-Rab7- and RLucII-Rab7-expressing cells compared to untransfected cells (Fig. S1C). The recruitment efficiency of Myc-Rab7 and RLucII-Rab7 were comparable as Vps35 intensity in the two conditions was not significantly different (Fig. S1C).

To determine whether palmitoylation plays a role in modulating interaction between Rab7 and retromer, HEK-293 cells were cotransfected with a constant amount of RLucII-Rab7 or RLucII-Rab7$_{C83,84S}$, and increasing concentrations of Vps26A-GFP10 or RILP-GFP10, to generate BRET titration curves (Kobayashi et al., 2009; Mercier et al., 2002). The BRET signal between RLucII-Rab7 and Vps26A-GFP10 rapidly increased with increasing amounts of expressed Vps26A-GFP10 until it reached saturation (Fig. 5A, black line), suggestive of a specific interaction (Mercier et al., 2002). By contrast, RLucII-Rab7$_{C83,84S}$ displayed a lower BRET value with Vps26A-GFP10 that never fully reaches saturation (Fig. 5A, blue line). As a control, we tested the interaction of Rab1a (RLucII-Rab1a), which localizes to the Golgi complex, with retromer. As expected, we found no interaction, as demonstrated by a linear curve (Fig. 5A, red line). Conversely, we tested the interaction between Rab7 and the µ1 (µ1-GFP10) subunit of the AP-1 family of clathrin adaptors. Once again, we did not detect an interaction (Fig. 5A, green line), suggesting that the BRET curves between Rab7 and retromer represent a specific interaction. BRET$_{50}$ is the value at which the concentration of the acceptor is required to obtain 50% of the maximal BRET signal (BRET$_{MAX}$) and is indicative of the propensity for the donor and acceptor to interact (Kobayashi et al., 2009; Mercier et al., 2002). We calculated BRET$_{50}$ for the interaction between wild-type Rab7 or Rab7$_{C83,84S}$ and Vps26A, and found a fourfold increase in the BRET$_{50}$ value for Rab7$_{C83,84S}$ binding to Vps26A (Fig. 5A, black bar) compared to wild-type Rab7 (Fig. 5A, gray bar), suggesting a much weaker interaction. Interestingly, palmitoylation of Rab7 did not appear to modulate the Rab7/RILP interaction, as we found no significant changes in the BRET titration curves between Rab7 and RILP (Fig. 5B, black line), or Rab7$_{C83,84S}$ and RILP (Fig. 5B, blue line), or the BRET$_{50}$ of these interactions (Fig. 5B, gray and black bars). As expected,

Journal of Cell Science (2017) 130, 2579-2590 doi:10.1242/jcs.199729

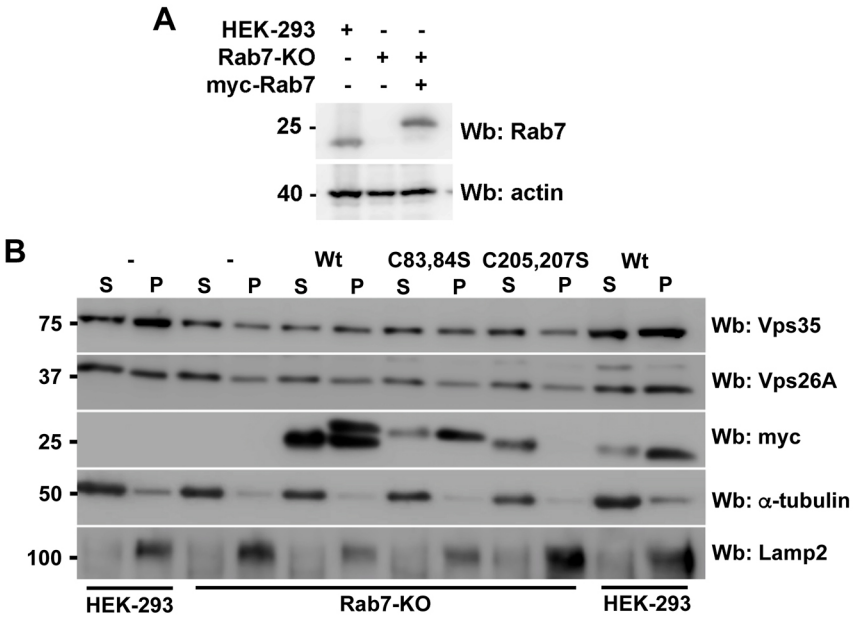

Fig. 3. Rab7 palmitoylation is required for retromer recruitment. (A) Whole cell lysates of HEK-293, Rab7-KO cells (generated using CRISPR-Cas9), or Rab7-KO cells transiently transfected with Myc-Rab7, were analyzed via WB with anti-Rab7 antibody. Anti-actin staining was used as a loading control. (B) HEK-293 or Rab7-KO cells were transfected with Myc-Rab7 and the indicated mutants. 48 h post-transfection, a membrane separation assay was performed and samples were subjected to WB with anti-Myc, anti-Vps26A, anti-Vps35, anti-α-tubulin (a cytosolic marker) and anti-Lamp2 (a membrane marker) antibodies.

Rab1a did not interact with RILP (Fig. 5B, red line). These data show that even if the palmitoylation-deficient mutant is still membrane bound, its interaction with Vps26A is significantly less efficient than that of wild-type Rab7. However, it would appear that not all interactions between Rab7 and effectors are modulated by palmitoylation, suggesting that this post-translational modification can mediate specific Rab7 functions.

To further explore how palmitoylation mediates the Rab7-retromer interaction, we performed a co-immunoprecipitation (co-IP) experiment by expressing wild-type Myc-Rab7, the nonpalmitoylatable mutant Myc-Rab7$_{C83,84S}$ and (HA)$_3$-Vps35 separately in HEK-293 cells. We then mixed lysates from each of the Rab7-expressing cells with lysate from cells expressing (HA)$_3$-Vps35 and performed co-IP using anti-HA antibody. If palmitoylation modulates the conformation of Rab7 to enable an interaction with retromer, Myc-Rab7$_{C83,84S}$ would not bind (HA)$_3$-Vps35 in this assay. On the other hand, if palmitoylation is required to localize Rab7 to facilitate an interaction with retromer, we would expect an interaction in this assay since the proteins are in a lysate and not membrane localized. We found an interaction between Myc-Rab7 and (HA)$_3$-Vps35, and between Myc-Rab7$_{C83,84S}$ and (HA)$_3$-Vps35 (Fig. S2), suggesting that the role of palmitoylation is to localize Rab7 to a specific endosomal domain leading to an optimal interaction with retromer. As expected, (HA)$_3$-Vps35 also interacted with another retromer subunit, Vps26A (Fig. S2).

Retromer is not efficiently localized to Rab7$_{C83,84S}$ puncta

To determine whether palmitoylation is required to localize Rab7 to endosomal domains, thereby modulating the Rab7-retromer interaction, we transfected U2OS cells with Myc-Rab7 (Fig. 5C, D, green) or Myc-Rab7$_{C83,84S}$ (Fig. 5E,F, green), to evaluate colocalization between these proteins and endogenous Vps26A (Fig. 5A-D, red) using structured illumination microscopy (SIM). Colocalization between Myc-Rab7 or Rab7$_{C83,84S}$ and Vps26A was determined using Mander's coefficient. We determined the amount of Vps26A colocalizing with wild-type Rab7 or Rab7$_{C83,84S}$ puncta, and observed reduced colocalization between Vps26A and Rab7$_{C83,84S}$ (Fig. 5E,F,G, black bars) compared to Myc-Rab7 (Fig. 5C,D,G, white bars). We then compared the amount of Rab7 localized to Vps26A puncta between wild-type Rab7 and Rab7$_{C83,84S}$ (Fig. 5G, white bars), and found a slight, but statistically significant, decrease in the degree of colocalization observed in the Rab7$_{C83,84S}$ mutant. Indeed, Rab7 is required to recruit Vps26A to endosomes (Rojas et al., 2008), thus it is expected that Rab7 will be present in Vps26A-positive puncta on endosomes. However, these data suggest that loss of palmitoylation does not completely prevent interaction between Rab7 and retromer but, due to reduced interaction ability, nonpalmitoylatable Rab7 is not as efficient at recruiting retromer to endosomal membranes.

Rab7$_{C83,84S}$ is less efficient at coordinating retromer cargo receptor retrieval

Since Rab7 palmitoylation is required for an optimal interaction with retromer CSC, we hypothesized that the absence of palmitoylation would result in decreased retromer function. In humans and yeast, altered retromer function is associated with impaired trafficking of lysosomal/vacuolar enzymes that results in their secretion into the extracellular space (Bonangelino et al., 2002; Follett et al., 2016; Rojas et al., 2008). We asked if Rab7 palmitoylation is required for the correct trafficking of the lysosomal enzyme cathepsin D. To test the effect of Rab7 palmitoylation on cathepsin D trafficking, we compared the secretion of cathepsin D in HEK-293 cells, Rab7-KO cells and Rab7-KO cells transiently expressing wild-type Myc-Rab7 and the various mutants (Fig. 6A). As expected, in HEK-293 cells, cathepsin D is correctly trafficked to the lysosome with almost no secretion of the protein into the medium (Fig. 6A). Rab7-KO cells are not able to efficiently recruit retromer to endosomes, resulting in inefficient trafficking of the lysosomal sorting receptors and the secretion of cathepsin D (Fig. 6A). The expression of Myc-Rab7 in Rab7-KO cells rescues cathepsin D trafficking; therefore, secretion is reduced compared to Rab7-KO cells (Fig. 6A). The expression of the prenylation mutant (Rab7$_{C205,207S}$) does not rescue Rab7-KO cells, resulting in secretion of cathepsin D (Fig. 6A). Expression of Myc-Rab7$_{C83,84S}$ does not efficiently rescue cathepsin D secretion, suggesting that efficient lysosomal localization of this protease is dependent on Rab7 palmitoylation (Fig. 6A). Functionally, palmitoylation of Rab7 plays a significant

Journal of Cell Science (2017) 130, 2579-2590 doi:10.1242/jcs.199729

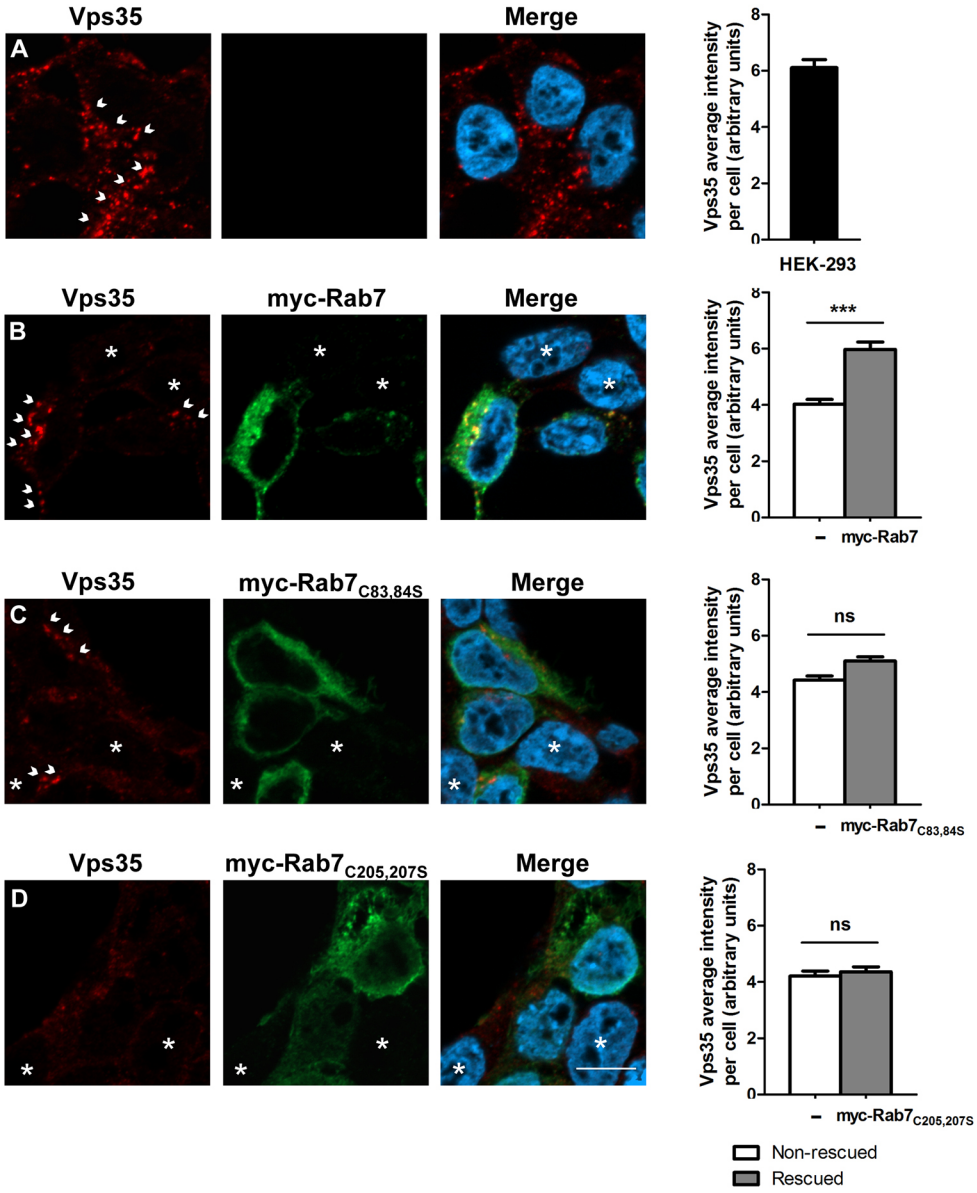

Fig. 4. Rab7$_{C83,84S}$ is not efficient at recruiting retromer to endosomes. (A) HEK-293 cells were fixed with 4% PFA and immunostained with anti-Vps35 antibody (red, arrowheads). Graph shows the average Vps35 puncta intensity in HEK-293 cells (black bar). Data are mean±s.e.m. (B) Rab7-KO cells were transfected with Myc-Rab7. 24 h post-transfection, cells were fixed with 4% PFA and immunostained with anti-Myc (green) and anti-Vps35 antibodies (red, arrowheads). Fluorescence intensity of Vps35 puncta from 55 transfected and 59 nontransfected cells (asterisks) was determined. Graph shows the average Vps35 puncta intensity in Rab7-KO cells (white bar) and Rab7-KO cells expressing Myc-Rab7 (gray bar). Data are mean±s.e.m. ***P<0.0001 (two-tailed unpaired t-test). (C) Same procedures as in B, except cells were transfected with Myc-Rab7$_{C83,84S}$. Fluorescence intensity of Vps35 puncta from 57 transfected and 57 nontransfected cells (asterisks) was determined. Graph shows the average intensity of Vps35 puncta in Rab7-KO cells (white bar) and Rab7-KO cells expressing Myc-Rab7$_{C83,84S}$ (gray bar). Data are mean±s.e.m. ns, not significant. (D) Same procedures as in B, except cells were transfected with Myc-Rab7$_{C205,207S}$. Fluorescence intensity of Vps35 puncta from 58 transfected and 57 nontransfected cells (asterisks) was determined. Graph shows the average Vps35 puncta intensity in Rab7-KO cells (white bar) and Rab7-KO cells expressing Myc-Rab7$_{C205,207S}$ (gray bar). Data are mean±s.e.m. ns, not significant. Scale bar: 10 µm.

role in modulating efficient endosome-to-TGN trafficking of the lysosomal sorting receptors and the proper localization of lysosomal proteins.

Rab7 palmitoylation is not required for degradation of integral membrane proteins

Although Rab7 is required for the spatiotemporal recruitment of retromer and therefore efficient endosome-to-TGN trafficking of CI-MPR (also known as IGF2R) and sortilin, it also regulates the degradation of integral membrane proteins such as EGFR (Shinde and Maddika, 2016; Vanlandingham and Ceresa, 2009). Upon stimulation with epidermal growth factor (EGF), EGFR is internalized and degraded in lysosomes (Futter et al., 1996). We stimulated cells that had been previously incubated for 1 h with cycloheximide and 100 ng/ml EGF for either 15 or 120 min and compared the degradation of EGFR in HEK-293, Rab7-KO and Rab7-KO cells expressing wild-type Myc-Rab7, Myc-Rab7$_{C83,84S}$ or Myc-Rab7$_{C205,207S}$. Nonstimulated (NS) cells served as controls. As expected, HEK-293 cells and HEK-293 cells overexpressing Myc-Rab7 efficiently degrade EGFR following stimulation with EGF (Fig. 6B). However, compared to HEK-293 cells, Rab7-KO cells are not able to degrade EGFR as efficiently (Fig. 6B), while Rab7-KO cells expressing Myc-Rab7 can. Rab7-KO cells expressing Myc-Rab7$_{C83,84S}$ appear to degrade some EGFR but with slower degradation kinetics (at 15 min chase) compared to HEK-293 cells, while Rab7-KO cells expressing Myc-Rab7$_{C205,207S}$ also presented significant delay.

EGF is efficiently degraded in Rab7-KO cells expressing Myc-Rab7$_{C83,84S}$

Although EGFR degradation was partially restored in Rab7-KO cells expressing Myc-Rab7$_{C83,84S}$, the degradation assay determines the amount of EGFR remaining in all cells, not just in cells that have been rescued. To support our EGFR degradation data, we tested the degradation of EGF labeled with Alexa Fluor 488 (EGF-488) so that we could evaluate degradation in rescued cells specifically. Cells were incubated with 300 ng EGF-488 for 30 min, washed and then chased for 0, 15 and 60 min. In HEK-293 cells, we found very little EGF-488 as it was efficiently degraded (Fig. 7A,F,K). Quantification of 20 cells revealed that, on average, HEK-293

Journal of Cell Science (2017) 130, 2579-2590 doi:10.1242/jcs.199729

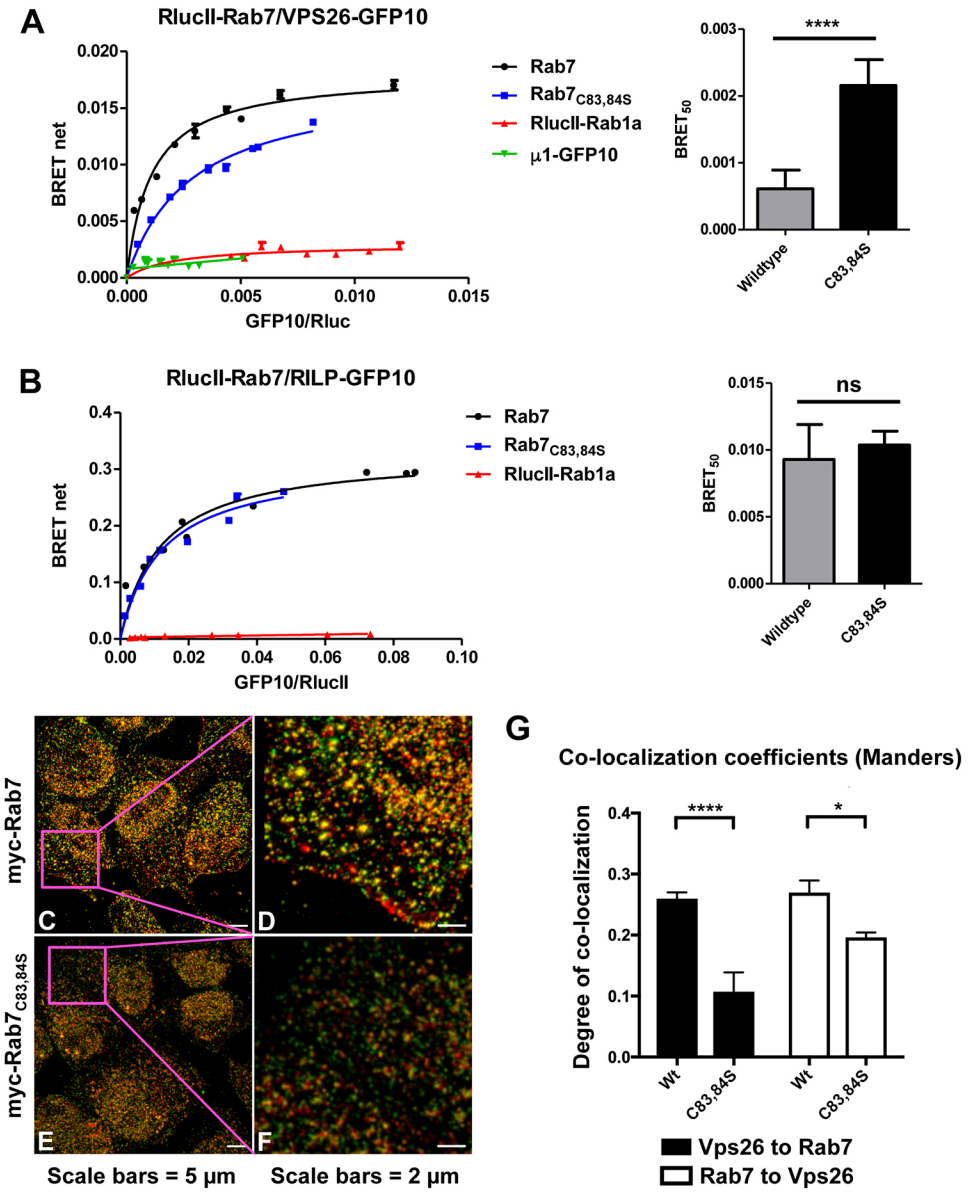

Fig. 5. Palmitoylation modulates the interaction between Rab7 and retromer. (A) HEK-293 cells were transfected with a constant amount of RLucII-Rab7, RLucII-Rab7$_{C83,84S}$ or RLucII-Rab1a, and increasing amounts of Vps26A-GFP10 or μ1-GFP10. 48 h post-transfection BRET analysis was performed. BRET signals are plotted as a function of the ratio between the GFP10 fluorescence and RLucII luminescence. BRET$_{50}$, concentration of the acceptor required to obtain 50% of BRET$_{MAX}$. In A and B, data are mean±s.d. from three experiments. ns, not significant; ****P<0.0001 (two-tailed paired t-test). (B) HEK-293 cells were transfected with a constant amount of RLucII-Rab7, RLucII-Rab7$_{C83,84S}$ or RLucII-Rab1a, and increasing amounts of RILP-GFP10. (C-F) U2OS cells were transiently transfected with Myc-Rab7 (C,D) or Rab7$_{C83,84S}$ (E,F), immunostained with anti-Myc (green, C-F) and anti-Vps26A (red, C-F) antibodies, and analyzed via SIM. D,F are magnified images of the boxed areas in C,E, respectively. (G) Cells were analyzed for colocalization (10–20 cells per condition) and the average Mander's colocalization coefficient was calculated. Data are mean ±s.e.m. *P<0.05; ****P<0.0001 (two-tailed unpaired t-test).

cells contained 4.15, 4.35 and 3.2 EGF-488 puncta at 0, 15 and 60 min, respectively (Fig. 7P, white bars). In Rab7-KO cells, we observed a significant increase in the amount of EGF-488 puncta (Fig. 7B,G,L, asterisks), and quantification revealed 10.65, 10.85 and 9.8 EGF-488 puncta at 0, 15 and 60 min, respectively (Fig. 7P, black bars). Expressing wild-type Myc-Rab7 reduced the number of EGF-488 puncta in Rab7-KO cells (Fig. 7C,H,M) to levels comparable to HEK-293 cells (Fig. 7P, gray bars). Supporting our EGFR degradation data (Fig. 6B), expressing Myc-Rab7$_{C83,84S}$ in Rab7-KO cells also decreased the number of EGF-488 puncta to levels comparable to HEK-293 cells (Fig. 7D,I,N). Quantification of 20 cells revealed no significant difference in the number of puncta (4.4, 5.65, 4.65 at 0, 15 and 60 min, respectively) in Rab7-KO expressing Myc-Rab7$_{C83,84S}$ compared to HEK-293 cells (Fig. 7P, diagonal striped bars). Cells that do not express Myc-Rab7$_{C83,84S}$ in the same field of view accumulated EGF-488 puncta (Fig. 7D,N, asterisks). As expected, expression of Myc-Rab7$_{C205,207S}$ in Rab7-KO cells (Fig. 7E,J,O) had no effect on the number of EGF-488 puncta (Fig. 7P, horizontal striped bars) as these cells contained an average of 8.7, 9.5 and 10.7 puncta at 0, 15 and 60 min, respectively.

DISCUSSION

Rabs are key regulators of the formation, trafficking, and fusion of transport vesicles at the endoplasmic reticulum (ER), Golgi complex, and early and late endosomes (Hutagalung and Novick, 2011). Rab7 functions in many pathways at endosomes, including the recruitment of retromer (Rojas et al., 2008; Seaman et al., 2009) and the recruitment of RILP (Cantalupo et al., 2001), and mediates the fusion of lysosomes with autophagosomes via the homotypic fusion and protein sorting (HOPS) complex (McEwan et al., 2015). The molecular mechanisms that regulate and determine these various functions of Rab7 are not well understood. Here, we demonstrate that Rab7 is palmitoylated, and that this post-translational modification plays a role in mediating the function of Rab7 in retromer recruitment and therefore in regulating endosome-to-TGN traffic.

Rab7 is palmitoylated on two cysteine residues

Rab7 and Ypt7 have four conserved cysteine residues. Two of these are the C-terminal cysteines that are prenylated, C205 and C207 in mammalian Rab7, and C206 and C208 in yeast Ypt7. As we have

Journal of Cell Science (2017) 130, 2579-2590 doi:10.1242/jcs.199729

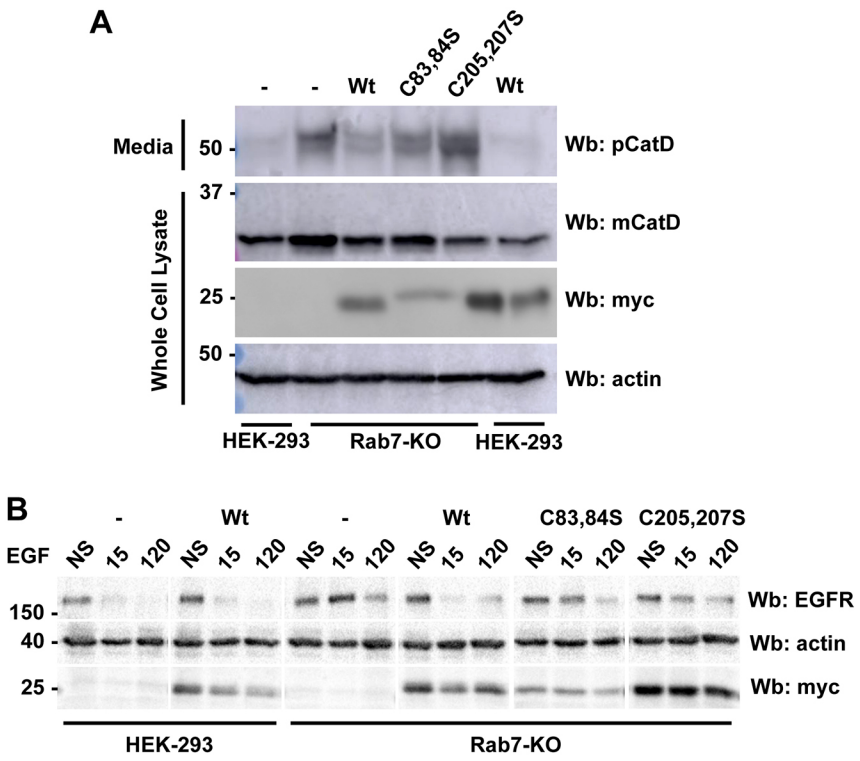

Fig. 6. Rab7$_{C83,84S}$ is not efficient at regulating endosome-to-TGN cargo receptor retrieval. (A) HEK-293 or Rab7-KO cells were transfected with wild-type Myc-Rab7 or the indicated mutants. 48 h post-transfection, the medium was changed to Opti-MEM supplemented with cycloheximide and collected after 4.5 h. Proteins were precipitated and resuspended in Laemmli buffer (conditioned medium). Whole cell lysate and conditioned medium were run on a 12% polyacrylamide gel and WB was performed with anti-cathepsin D, anti-Myc and anti-actin antibodies. (B) HEK-293 or Rab7-KO cells were transfected as indicated. After a 1 h treatment with 50 µg/ml cycloheximide to prevent *de novo* protein synthesis, cells were treated with 100 ng/ml EGF for either 15 or 120 min. Nonstimulated (NS) cells served as a control. After EGF stimulation, the cells were lysed and whole cell lysate was run on a 12% polyacrylamide gel, transferred to nitrocellulose membrane, and WB was performed using anti-EGFR, anti-actin and anti-Myc antibodies.

shown (Fig. 1C), these terminal residues are required for membrane anchoring. The other conserved cysteines are found between Switch I and Switch II, C83 and C84 in mammalian Rab7, and C84 and C85 in yeast Ypt7. We now demonstrate that these residues in Rab7 are palmitoylated. Rab7$_{C205,207S}$ is not palmitoylated and we suggest that membrane anchoring is a prerequisite for palmitoylation. The palmitoyltransferases (PATs), of which 24 have been found in humans and seven in yeast, are all multispan integral membrane proteins (Linder and Deschenes, 2007). We propose that prenylation enables Rab7 to anchor into endosomal membranes. Subsequently, a subpopulation could be palmitoylated by one or more PATs. Further work will be required to identify the mechanism of Rab7 palmitoylation. The PAT DHHC5 is an excellent candidate as endosome-to-TGN trafficking was disrupted in cells depleted of DHHC5 by RNAi (Breusegem and Seaman, 2014). Furthermore, DHHC5 localizes to endosomes and could serve as a local mechanism for Rab7 palmitoylation.

Rab7 palmitoylation mediates its interaction with a subset of downstream effectors

Palmitoylation does not act as a membrane anchor for Rab7, but rather it modulates interactions. Using BRET, we found that Rab7$_{C83,84S}$ bound significantly less retromer than wild-type Rab7. However, RILP bound equally well to both wild-type Rab7 and Rab7$_{C83,84S}$. It will be interesting to determine how palmitoylation of Rab7 mediates interaction with other effectors such as HOPS, Rubicon and PLEKHM1. Based on our data, we find that palmitoylation modulates Rab7 function and its interaction with retromer by localizing the protein into specific endosomal subdomains, and probably not by regulating its GTP-bound status.

Rab7 post-translational modifications

It is becoming more apparent that the function of Rab7 is modified and regulated by post-translational modifications. We have demonstrated that Rab7 palmitoylation is required for the efficient endosome-to-TGN trafficking of the lysosomal sorting receptors. Recent studies have also shown how phosphorylation (Francavilla et al., 2016; Shinde and Maddika, 2016) and ubiquitination (Song et al., 2016) can regulate Rab7 function. Rab7 has at least two phosphorylation sites (serine 72 and tyrosine 183), which can act as a negative regulator or modulate function. Indeed, phosphorylation at serine 72 acts as an 'off switch' for Rab7 as the phosphomimetic mutant was completely cytosolic (Shinde and Maddika, 2016), while phosphorylation at tyrosine 183 is required to mediate the degradation of the EGFR (Francavilla et al., 2016). Here, we demonstrate that palmitoylation also regulates the function of Rab7. As far as we know, we are the first to confirm this post-translational modification on a mammalian Rab protein and the first to functionally characterize the role of palmitoylation on the function of a Rab. It will be interesting to confirm palmitoylation of other Rabs and elucidate how this modification would affect their function. Our work adds another regulatory mechanism to Rab7 biology. By combining phosphorylation, ubiquitination and palmitoylation, cells can modulate Rab7 function to various pathways and modulating these mechanisms could prove to be valuable targets in diseases in which Rab7 is implicated.

MATERIALS AND METHODS

Antibodies and reagents

Unless otherwise stated, all reagents were purchased from Fisher Scientific. The following mouse monoclonal antibodies were used: anti-Myc 9E10 (MMS-150P, Cedarlane Laboratories), anti-Vps35 (ab57632, Abcam), anti-actin Ab5 (612657, BD Biosciences), anti-α-tubulin (T9026, Sigma-Aldrich), anti-Lamp-2 (ab25631, Abcam), anti-Renilla luciferase (MAB4400, Fisher Scientific) and anti-HA (16B12, Cedarlane Laboratories). The following rabbit polyclonal antibodies were used: anti-Vps26A (ab23892, Abcam), anti-TRAPPC3 (15555-1-AP, Cedarlane Laboratories), anti-RILP (ab128616, Abcam), anti-Myc (2272, Cell Signaling Technology) and anti-FLAG (F7425, Sigma-Aldrich). The following rabbit monoclonal antibodies were used: anti-Rab7 (D95F2, Cell Signaling Technology), and anti-EGFR (ab52894, Abcam). All

Journal of Cell Science (2017) 130, 2579-2590 doi:10.1242/jcs.199729

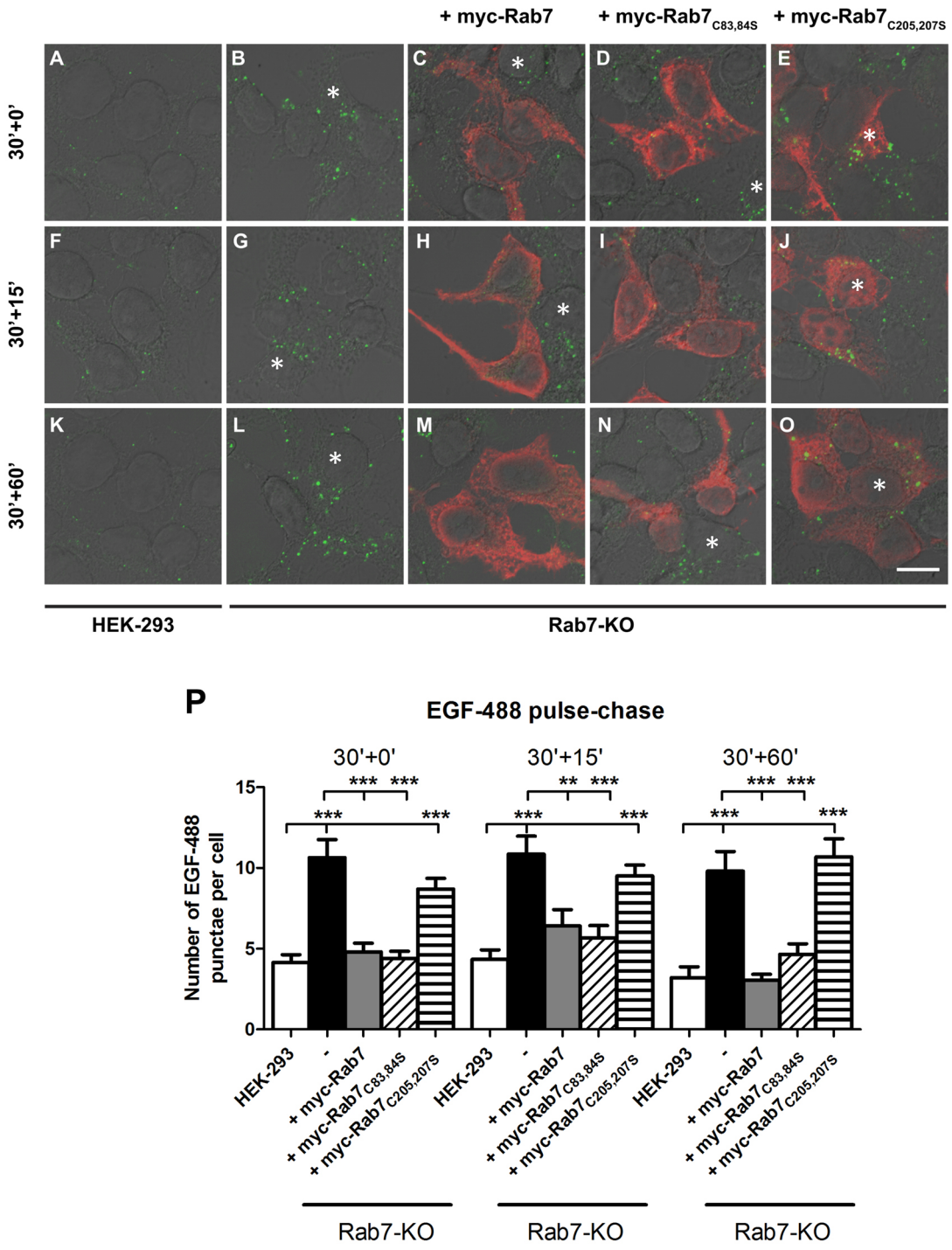

Fig. 7. Rab7 palmitoylation is not required for EGF degradation. (A-O) HEK-293 (A,F,K), Rab7-KO cells (B,G,L), Rab7-KO cells transiently expressing Myc-Rab7 (C,H,M), Myc-Rab7$_{C83,84S}$ (D,I,N) or Myc-Rab7$_{C205,207S}$ (E,J,O) were incubated with 300 ng Alexa Fluor 488-tagged EGF and chased for the indicated times. Representative images are shown. Cells accumulating EGF-488 that are not expressing Rab7 or one of the Rab7 mutants are indicated (asterisks). Scale bar: 10 µm. (P) Quantification of EGF-488 puncta (20 cells were analyzed per condition). Data are mean±s.d. $^{**}P<0.01$; $^{***}P<0.0001$ (one-way ANOVA with Tukey's post-hoc test).

antibodies were used at a dilution of 1:1000 for WB and IF except anti-Myc, which was used at 1:500 for IF, and Lamp-2, which was used at 1:500 for WB.

Cloning and mutagenesis

All restriction enzymes used for cloning were purchased from New England Biolabs. Vps29-(FLAG)$_3$ was generated by amplifying Vps29 cDNA from Vps29-YFP via PCR and cloned into BstbI/NotI of pEZ-M14 (GeneCopoeia). For Myc-Rab7, the cDNA of Rab7 was amplified from RFP-Rab7 (a gift from Ari Helenius, plasmid #14436, Addgene) via PCR and cloned into the XbaI/NheI sites of pKMyc (a gift from Ian Macara, plasmid #19400, Addgene). All the mutants described were generated via PCR mutagenesis using cloned PFU polymerase (Agilent Technologies). RLucII-Rab7 and RLucII-Rab7$_{C83,84S}$ were generated by amplifying Rab7 cDNA from Myc-Rab7 and Myc-Rab7$_{C83,84S}$ and cloned into the EcoRV/XhoI site of pcDNA3.1 Hygro (+) RLucII-GFP10-st2 plasmid. To obtain

Journal of Cell Science (2017) 130, 2579-2590 doi:10.1242/jcs.199729

Vps26A-GFP10, Vps26A cDNA was amplified from Vps26A-YFP and cloned into the NheI/BamHI sites of pcDNA3.1 Hygro (+)-GFP10-RLucII. RLucII-Rab1a was generated by amplifying Rab1a cDNA from Myc-Rab1a (a gift from Dr Terry Hebert, McGill University, Montreal, Canada) and cloned into the EcoRV/XhoI sites of pcDNA3.1 Hygro (+) RLucII-GFP10-st2 plasmid. pcDNA3.1 Hygro (+) RLucII-GFP10-st2 and pcDNA3.1 Hygro (+) GFP10-RLucII-st2 plasmids were generous gifts from Dr Michel Bouvier (IRIC, Université de Montreal, Montreal, Canada). RILP-GFP10 was generated by amplifying RILP cDNA from HA-RILP (a generous gift from Cecilia Bucci, University of Salento, Lecce, Italy) and cloned into the NheI/KpnI sites of pcDNA3.1 Hygro (+)-GFP10-RLucII.

Cell culture

Cells were maintained in Dulbecco's modified Eagle's medium (DMEM) supplemented with 10% fetal calf serum and penicillin-streptomycin (Thermo Fisher Scientific). All cells were originally obtained from ATCC and periodically checked for contamination. All transfections, unless otherwise noted, were performed with polyethylenimine (PEI) (Thermo Fisher Scientific). Briefly, solution A was prepared diluting plasmid into Opti-MEM (Thermo Fisher Scientific). Solution B was prepared by diluting PEI (1 µg/µl) in Opti-MEM in a 1:3 ratio with the DNA to transfect. After 5 min incubation, the two solutions were mixed, vortexed for 3 s, incubated at room temperature (RT) for 15 min and added to the cells.

Acyl-RAC to isolate palmitoylated proteins

The protocol to detect palmitoylated protein was adapted from a published protocol (Ren et al., 2013). Briefly, protein lysates were incubated overnight at RT with 0.5% methyl methanethiosulfonate (MMTS) (Sigma-Aldrich) to block free cysteine residues. Proteins were then precipitated by adding two volumes of cold acetone and incubated at −20°C for 2 h. After washing with cold acetone, the pellet was resuspended in binding buffer (100 mM HEPES, 1 mM EDTA, 1% SDS). Water-swollen thiopropyl Sepharose 6B (GE Healthcare Life Sciences) was added and samples were divided into two equal parts. One part was treated with hydroxylamine (Sigma-Aldrich), pH7.5, to a final concentration of 0.2 M to cleave palmitate residues from proteins; the other part was treated with an equal amount of NaCl as a control. After 3 h incubation at RT, beads were washed five times with binding buffer and captured proteins were eluted with 75 mM DTT.

Membrane separation assay

24 h post-transfection, cells were harvested, snap frozen with liquid nitrogen and allowed to thaw at room temperature. Samples were resuspended in buffer 1 (0.1 M Mes-NaOH, pH 6.5, 1 mM MgAc, 0.5 mM EGTA, 200 µM sodium orthovanadate, 0.2 M sucrose) and centrifuged at 10,000 ***g*** for 5 min at 4°C. The supernatant containing cytosolic proteins was collected (S, soluble fraction) and the pellet was resuspended in buffer 2 (50 mM Tris-HCl, 150 mM NaCl, 1 mM EDTA, 0.1% SDS, 1% Triton X-100) and spun at 10,000 ***g*** for 5 min at 4°C. The supernatant containing membrane proteins was collected (P, pellet fraction) for further analysis. Equal volumes of each fraction were loaded for WB. The intensity of the bands on blots was determined using Fiji (Schindelin et al., 2012). Analysis of the distribution of proteins between the two fractions was performed by dividing the intensity of each fraction by the total in each condition and expressed as a percentage.

CRISPR-Cas9 Rab7-KO cell line

HEK-293 were transfected with an all-in-one CRISPR plasmid for Rab7 (plasmid #HTN218819, GeneCopoeia). 72 h post-transfection, cells were treated with 1 mg/ml Geneticin (Thermo Fisher Scientific) for 1 week. Limiting dilution was performed to isolate single cells. Single clones were allowed to grow for approximately 2 weeks prior to testing via immunoblotting to identify Rab7-KO clones.

Immunofluorescence microscopy

HEK-293 or U2OS cell IF was performed as previously described (Dumaresq-Doiron et al., 2010). Briefly, cells were seeded on glass coverslips overnight and subsequently transiently transfected with indicated plasmids. 48 h post-transfection, cells were washed once in PBS, fixed with 4% paraformaldehyde in PBS for 15 min at RT and washed twice with PBS. Cells were permeabilized with 0.1% Triton X-100, 1% bovine serum albumin (BSA) (Fisher Scientific) in PBS for 5 min at RT, washed once with PBS, and incubated for 2 h with primary antibodies in a solution of 0.1% BSA in PBS. Cells were then washed three times in PBS and incubated for 1 h at RT with appropriate secondary antibodies conjugated to either Alexa Fluor 594 (Thermo Fisher Scientific) or Alexa Fluor 488 in a solution of 0.1% BSA in PBS. Cells were washed once with PBS and incubated with DAPI (Thermo Fisher Scientific) in PBS for 5 min at RT. Cells were then washed three times with PBS and mounted on glass slides with Fluoromount G (Fisher Scientific). Quantification of fluorescence intensity was performed using Fiji software by manually outlining nonrescued or rescued Rab7-KO cells. Quantification of colocalization was performed using the Fiji plugin Coloc2 by manually outlining the double-labeled cells.

BRET assay

BRET assay was performed as previously described (Gales et al., 2006; Kobayashi et al., 2009). Briefly, HEK-293 cells were seeded in 12-well plates (Fisher Scientific) and transfected with the indicated plasmids. 48 h post-transfection, cells were washed once with PBS, detached with 5 mM EDTA in PBS and resuspended in 500 µl PBS. Cell suspensions were distributed into 96-well plates (Fisher Scientific); each sample was plated in triplicate. BRET signal was measured after the addition of the RLucII substrate DeepBlueC coelenterazine (Cedarlane Laboratories) to a final concentration of 5 µM. Readings were performed using an Infinite M1000Pro (Tecan). The BRET signal was calculated as a ratio between GFP10 emission (500–535 nm) over RLucII emission (370–450 nm). The BRET net signal was calculated as the difference between the total BRET signals and the one obtained from experiments in which only the RLucII is expressed. The expression level of Vps26A-GFP10 was measured by reading the emission of fluorescence at 510 nm after exciting the fluorophore at 400 nm. The expression level of RLucII was measured by reading the emission at 370–450 nm after the addition of the substrate. BRET signal was plotted as function of GFP10 fluorescence over RLucII luminescence (GFP10/RLuc).

SIM

U2OS cells were seeded in eight-well LabTek #1.5 borosilicate chambered coverglass imaging dishes (Fisher Scientific) to 50–60% confluency. Wild-type Myc-Rab7 and Myc-Rab7$_{C83,84S}$ were transiently expressed for 36 h in separate wells. Cells were then fixed with 2% paraformaldehyde (PFA) at 22°C for 20 min. Fixed cells were washed three times with 25 mM ammonium chloride (NH_4Cl) and 50 mM glycine to remove excess PFA and reduce autofluorescence, and then three times with PBS. The cells were permeabilized with 0.1% (v/v) Triton X-100 in PBS and blocked with 10% FBS (v/v) in PBS. Immunostaining was performed using anti-Myc and anti-Vps26A antibodies. An anti-mouse Alexa Fluor 488-conjugated secondary antibody (Thermo Fisher Scientific) and an anti-rabbit Alexa Fluor 647-conjugated secondary antibody (Thermo Fisher Scientific) were then used to indirectly label proteins with green and far-red fluorescence, respectively. After immunostaining, cells were washed three times with PBS prior to imaging. Imaging of samples was performed using SIM on a Zeiss Elyra PS.1 superresolution inverted microscope. Samples were imaged at an effective magnification of 101× (63× objective+1.6× optovar tube lens) on an oil immersion objective. Typically, 10–20 slices (0.110 µm) were captured for each field of view for an imaging volume of ∼1.1–2.2 µm. A 647 nm (and subsequently 488 nm) laser line was directed into the microscope optical train via a multimode fiber coupler. The laser was passed through a diffraction grating, and a series of diffraction orders (−1, 0, +1) were projected onto the back focal plane of the objective. These wavefronts were collimated in the objective to create a 3D sinusoidal illumination pattern on the sample. The diffraction grating was then rotated and translated throughout the acquisition to create patterned offset images containing higher spatial frequency information compared to widefield imaging. Five lateral positions were acquired at each of three diffraction grating rotations (120°) for a total of 15 raw images per slice. SIM imaging with both the 488 nm and 647 nm laser was performed at 50 ms exposures with laser power varying between 3 and 10%, and a gain level of 60–80. Raw SIM

image stacks were processed with the Structured Illumination toolbar of the Zeiss Zen software. A series of parameters were set to generate an optical transfer function (OTF) used for 3D reconstruction. The noise filter for Wiener de-convolution was set to a value of −6.0, and the maximum isotropy option was left unselected to recover all available frequency information at exactly the 120° rotation angles. Super-resolution frequency weighting was set at 1.0. Negative values arising as an artifact of the Wiener filter were clipped to zero using the Baseline Cut option. Sectioning filters used to remove the 0 frequencies from the 0th order and nonshifted 1st order (+1, −1) were set to 100 and 83, respectively. Processed SIM images were then aligned via an affine transformation matrix of predefined values obtained using 100 nm multicolor Tetraspeck fluorescent microspheres (Thermo Fisher Scientific). Dual channel-aligned images were analyzed using the colocalization function in Zen. Regions of interest were drawn in the cytoplasm (omitting the nucleus) of 10–20 cells for each of the wild-type and mutant Rab7 cell types. The average Manders colocalization coefficients over the imaging volume were calculated for both channels. The average Manders colocalization coefficients and standard deviations were calculated across the sample size for wild-type and all mutants.

Cathepsin D secretion assay

A cathepsin D secretion assay was performed as previously described (Follett et al., 2016). Briefly, HEK-293 and Rab7-KO cells were transfected with the indicated plasmids. 48 h post-transfection, cells were incubated in serum-free medium (Opti-MEM) supplemented with 100 µg/ml cycloheximide and chased for 4.5 h. The medium was collected, precipitated with trichloroacetic acid, and the pellet was resuspended in Laemmli sample buffer. Cells were collected, and lysed in TNE (150 mM NaCl, 50 mM Tris-HCl, pH 7.5, 2 mM EDTA, 0.5% Triton X-100 and protease inhibitor cocktail) for 30 min on ice as previously described (Dumaresq-Doiron et al., 2013). The precipitated proteins collected from the medium and the cell lysate were then analyzed by WB.

EGFR degradation assay

HEK-293 or Rab7-KO cells were transfected with Myc-Rab7 and the various Rab7 mutants. 48 h post-transfection, the serum-starved cells were treated with 50 µg/ml cycloheximide for 1 h to prevent *de novo* synthesis of EGFR during EGF stimulation. Cells were subsequently stimulated with 100 ng/ml EGF for the indicated times, harvested and lysed in TNE as described above. The levels of EGFR were determined by WB.

EGF-488 pulse-chase experiments

Cells were seeded on coverslips. 24 h later, the cells were transfected with wild-type Myc-Rab7 or mutant constructs. 24 h post-transfection, cells were serum-starved in Opti-MEM for 1 h followed by a 30-min pulse of EGF-488 (ThermoFisher) at a concentration of 300 ng/ml. Cells were then washed with PBS and fixed in 4% paraformaldehyde at the following chase time points: 0, 15 or 60 min. Cells were immunostained with anti-Myc primary and Alexa Fluor 594-conjugated secondary antibodies. Cells were imaged using a Zeiss LSM 780 confocal microscope. The number of puncta per cell was counted manually (20 cells per condition for each time point).

Statistics

Statistical analysis was performed using GraphPad Prism Version 7. Statistical tests used are described in the corresponding figure legends.

Acknowledgements

We thank Dr Peter J. McCormick (University of Surrey, UK) for critical reading of the manuscript and helpful discussions.

Competing interests

The authors declare no competing or financial interests.

Author contributions

Conceptualization: G.M., H.W., S.L.; Methodology: G.M., O.S., E.S., A.V., P.K.K., H.W.; Formal analysis: G.M., O.S., E.S., A.V., P.K.K., H.W., S.L.; Investigation: O.S., E.S., A.V.; Writing - original draft: G.M., S.L.; Writing - review & editing: G.M., O.S., E.S., C.M.Y., P.K.K., H.W., S.L.; Supervision: C.M.Y., P.K.K., H.W., S.L.; Funding acquisition: H.W., S.L.

Funding

This work was supported by the Canadian Institutes of Health Research (MOP-10754 to S.L.; MOP-123438 to H.W.), Alzheimer Society (14-27 to S.L.), Fonds de Recherche du Québec - Santé (Junior 2 awards to S.L. and H.W.) and Natural Sciences and Engineering Research Council of Canada (post-doctoral fellowship to O.S.).

Supplementary information

Supplementary information available online at
http://jcs.biologists.org/lookup/doi/10.1242/jcs.199729.supplemental

References

Arighi, C. N., Hartnell, L. M., Aguilar, R. C., Haft, C. R. and Bonifacino, J. S. (2004). Role of the mammalian retromer in sorting of the cation-independent mannose 6-phosphate receptor. *J. Cell Biol.* **165**, 123-133.

Balderhaar, H. J., Arlt, H., Ostrowicz, C., Bröcker, C., Sündermann, F., Brandt, R., Babst, M. and Ungermann, C. (2010). The Rab GTPase Ypt7 is linked to retromer-mediated receptor recycling and fusion at the yeast late endosome. *J. Cell Sci.* **123**, 4085-4094.

Bonangelino, C. J., Chavez, E. M. and Bonifacino, J. S. (2002). Genomic screen for vacuolar protein sorting genes in Saccharomyces cerevisiae. *Mol. Biol. Cell* **13**, 2486-2501.

Breusegem, S. Y. and Seaman, M. N. J. (2014). Genome-wide RNAi screen reveals a role for multipass membrane proteins in endosome-to-golgi retrieval. *Cell Rep.* **9**, 1931-1945.

Burd, C. and Cullen, P. J. (2014). Retromer: a master conductor of endosome sorting. *Cold Spring Harb. Perspect. Biol.* **6**, a016774.

Cantalupo, G., Alifano, P., Roberti, V., Bruni, C. B. and Bucci, C. (2001). Rab-interacting lysosomal protein (RILP): the Rab7 effector required for transport to lysosomes. *EMBO J.* **20**, 683-693.

Chavrier, P., Gorvel, J.-P., Stelzer, E., Simons, K., Gruenberg, J. and Zerial, M. (1991). Hypervariable C-terminal domain of rab proteins acts as a targeting signal. *Nature* **353**, 769-772.

Cullen, P. J. (2008). Endosomal sorting and signalling: an emerging role for sorting nexins. *Nat. Rev. Mol. Cell Biol.* **9**, 574-582.

Dumaresq-Doiron, K., Savard, M.-F., Akam, S., Costantino, S. and Lefrancois, S. (2010). The phosphatidylinositol 4-kinase PI4KIIIalpha is required for the recruitment of GBF1 to Golgi membranes. *J. Cell Sci.* **123**, 2273-2280.

Dumaresq-Doiron, K., Jules, F. and Lefrancois, S. (2013). Sortilin turnover is mediated by ubiquitination. *Biochem. Biophys. Res. Commun.* **433**, 90-95.

Feinstein, T. N., Wehbi, V. L., Ardura, J. A., Wheeler, D. S., Ferrandon, S., Gardella, T. J. and Vilardaga, J.-P. (2011). Retromer terminates the generation of cAMP by internalized PTH receptors. *Nat. Chem. Biol.* **7**, 278-284.

Follett, J., Bugarcic, A., Collins, B. M. and Teasdale, R. D. (2017). Retromer's role in endosomal trafficking and impaired function in neurodegenerative diseases. *Curr. Protein Pept. Sci.* **7**, 687-701.

Follett, J., Bugarcic, A., Yang, Z., Ariotti, N., Norwood, S. J., Collins, B. M., Parton, R. G. and Teasdale, R. D. (2016). Parkinson's disease linked Vps35 R524W mutation impairs the endosomal association of retromer and induces alpha-synuclein aggregation. *J. Biol. Chem.* **291**, 18283-18298.

Forrester, M. T., Hess, D. T., Thompson, J. W., Hultman, R., Moseley, M. A., Stamler, J. S. and Casey, P. J. (2011). Site-specific analysis of protein S-acylation by resin-assisted capture. *J. Lipid Res.* **52**, 393-398.

Francavilla, C., Papetti, M., Rigbolt, K. T. G., Pedersen, A.-K., Sigurdsson, J. O., Cazzamali, G., Karemore, G., Blagoev, B. and Olsen, J. V. (2016). Multilayered proteomics reveals molecular switches dictating ligand-dependent EGFR trafficking. *Nat. Struct. Mol. Biol.* **23**, 608-618.

Futter, C. E., Pearse, A., Hewlett, L. J. and Hopkins, C. R. (1996). Multivesicular endosomes containing internalized EGF-EGF receptor complexes mature and then fuse directly with lysosomes. *J. Cell Biol.* **132**, 1011-1023.

Gales, C., Van Durm, J. J. J., Schaak, S., Pontier, S., Percherancier, Y., Audet, M., Paris, H. and Bouvier, M. (2006). Probing the activation-promoted structural rearrangements in preassembled receptor-G protein complexes. *Nat. Struct. Mol. Biol.* **13**, 778-786.

Gallon, M. and Cullen, P. J. (2015). Retromer and sorting nexins in endosomal sorting. *Biochem. Soc. Trans.* **43**, 33-47.

Haft, C. R., de la Luz Sierra, M., Bafford, R., Lesniak, M. A., Barr, V. A. and Taylor, S. I. (2000). Human orthologs of yeast vacuolar protein sorting proteins Vps26, 29, and 35: assembly into multimeric complexes. *Mol. Biol. Cell* **11**, 4105-4116.

Horazdovsky, B. F., Davies, B. A., Seaman, M. N., McLaughlin, S. A., Yoon, S. and Emr, S. D. (1997). A sorting nexin-1 homologue, Vps5p, forms a complex with Vps17p and is required for recycling the vacuolar protein-sorting receptor. *Mol. Biol. Cell* **8**, 1529-1541.

Hutagalung, A. H. and Novick, P. J. (2011). Role of Rab GTPases in membrane traffic and cell physiology. *Physiol. Rev.* **91**, 119-149.
Kang, R., Wan, J., Arstikaitis, P., Takahashi, H., Huang, K., Bailey, A. O., Thompson, J. X., Roth, A. F., Drisdel, R. C., Mastro, R. et al. (2008). Neural palmitoyl-proteomics reveals dynamic synaptic palmitoylation. *Nature* **456**, 904-909.
Kobayashi, H., Ogawa, K., Yao, R., Lichtarge, O. and Bouvier, M. (2009). Functional rescue of beta-adrenoceptor dimerization and trafficking by pharmacological chaperones. *Traffic* **10**, 1019-1033.
Kummel, D., Heinemann, U. and Veit, M. (2006). Unique self-palmitoylation activity of the transport protein particle component Bet3: a mechanism required for protein stability. *Proc. Natl. Acad. Sci. USA* **103**, 12701-12706.
Linder, M. E. and Deschenes, R. J. (2007). Palmitoylation: policing protein stability and traffic. *Nat. Rev. Mol. Cell Biol.* **8**, 74-84.
Liu, T.-T., Gomez, T. S., Sackey, B. K., Billadeau, D. D. and Burd, C. G. (2012). Rab GTPase regulation of retromer-mediated cargo export during endosome maturation. *Mol. Biol. Cell* **23**, 2505-2515.
Magee, T. and Newman, C. (1992). The role of lipid anchors for small G proteins in membrane trafficking. *Trends Cell Biol.* **2**, 318-323.
McEwan, D. G., Popovic, D., Gubas, A., Terawaki, S., Suzuki, H., Stadel, D., Coxon, F. P., Miranda de Stegmann, D., Bhogaraju, S., Maddi, K. et al. (2015). PLEKHM1 regulates autophagosome-lysosome fusion through HOPS complex and LC3/GABARAP proteins. *Mol. Cell* **57**, 39-54.
Mercier, J.-F., Salahpour, A., Angers, S., Breit, A. and Bouvier, M. (2002). Quantitative assessment of beta 1- and beta 2-adrenergic receptor homo- and heterodimerization by bioluminescence resonance energy transfer. *J. Biol. Chem.* **277**, 44925-44931.
Mitchell, D. A., Vasudevan, A., Linder, M. E. and Deschenes, R. J. (2006). Protein palmitoylation by a family of DHHC protein S-acyltransferases. *J. Lipid Res.* **47**, 1118-1127.
Progida, C., Spinosa, M. R., De Luca, A. and Bucci, C. (2006). RILP interacts with the VPS22 component of the ESCRT-II complex. *Biochem. Biophys. Res. Commun.* **347**, 1074-1079.
Ren, W., Jhala, U. S. and Du, K. (2013). Proteomic analysis of protein palmitoylation in adipocytes. *Adipocyte* **2**, 17-28.
Rocks, O., Peyker, A., Kahms, M., Verveer, P. J., Koerner, C., Lumbierres, M., Kuhlmann, J., Waldmann, H., Wittinghofer, A. and Bastiaens, P. I. (2005). An acylation cycle regulates localization and activity of palmitoylated Ras isoforms. *Science* **307**, 1746-1752.
Rojas, R., van Vlijmen, T., Mardones, G. A., Prabhu, Y., Rojas, A. L., Mohammed, S., Heck, A. J. R., Raposo, G., van der Sluijs, P. and Bonifacino, J. S. (2008). Regulation of retromer recruitment to endosomes by sequential action of Rab5 and Rab7. *J. Cell Biol.* **183**, 513-526.
Schindelin, J., Arganda-Carreras, I., Frise, E., Kaynig, V., Longair, M., Pietzsch, T., Preibisch, S., Rueden, C., Saalfeld, S., Schmid, B. et al. (2012). Fiji: an open-source platform for biological-image analysis. *Nat. Methods* **9**, 676-682.
Seaman, M. N. J. (2004). Cargo-selective endosomal sorting for retrieval to the Golgi requires retromer. *J. Cell Biol.* **165**, 111-122.
Seaman, M. N. J., Marcusson, E. G., Cereghino, J. L. and Emr, S. D. (1997). Endosome to Golgi retrieval of the vacuolar protein sorting receptor, Vps10p, requires the function of the VPS29, VPS30, and VPS35 gene products. *J. Cell Biol.* **137**, 79-92.
Seaman, M. N. J., McCaffery, J. M. and Emr, S. D. (1998). A membrane coat complex essential for endosome-to-Golgi retrograde transport in yeast. *J. Cell Biol.* **142**, 665-681.
Seaman, M. N. J., Harbour, M. E., Tattersall, D., Read, E. and Bright, N. (2009). Membrane recruitment of the cargo-selective retromer subcomplex is catalysed by the small GTPase Rab7 and inhibited by the Rab-GAP TBC1D5. *J. Cell Sci.* **122**, 2371-2382.
Shinde, S. R. and Maddika, S. (2016). PTEN modulates EGFR late endocytic trafficking and degradation by dephosphorylating Rab7. *Nat. Commun.* **7**, 10689.
Small, S. A. and Petsko, G. A. (2015). Retromer in Alzheimer disease, Parkinson disease and other neurological disorders. *Nat. Rev. Neurosci.* **16**, 126-132.
Song, P., Trajkovic, K., Tsunemi, T. and Krainc, D. (2016). Parkin modulates endosomal organization and function of the endo-lysosomal pathway. *J. Neurosci.* **36**, 2425-2437.
Steinberg, F., Gallon, M., Winfield, M., Thomas, E. C., Bell, A. J., Heesom, K. J., Tavaré, J. M. and Cullen, P. J. (2013). A global analysis of SNX27–retromer assembly and cargo specificity reveals a function in glucose and metal ion transport. *Nat. Cell Biol.* **15**, 461-471.
Temkin, P., Lauffer, B., Jäger, S., Cimermancic, P., Krogan, N. J. and von Zastrow, M. (2011). SNX27 mediates retromer tubule entry and endosome-to-plasma membrane trafficking of signalling receptors. *Nat. Cell Biol.* **13**, 717-723.
Vanlandingham, P. A. and Ceresa, B. P. (2009). Rab7 regulates late endocytic trafficking downstream of multivesicular body biogenesis and cargo sequestration. *J. Biol. Chem.* **284**, 12110-12124.

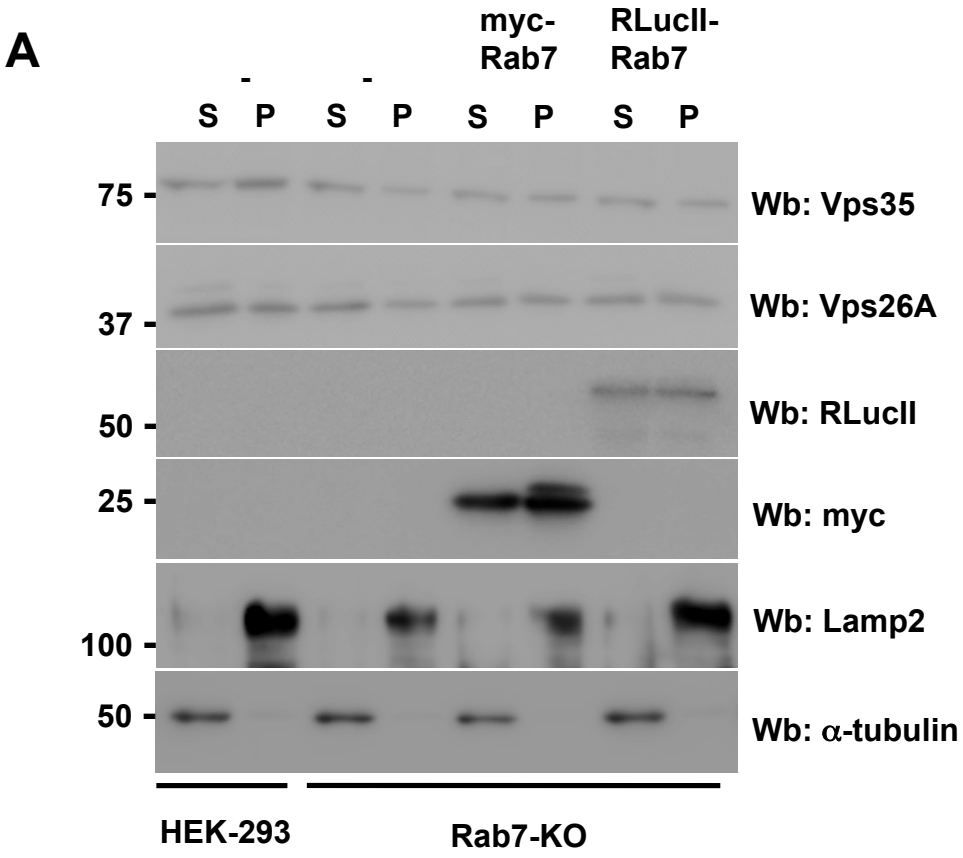

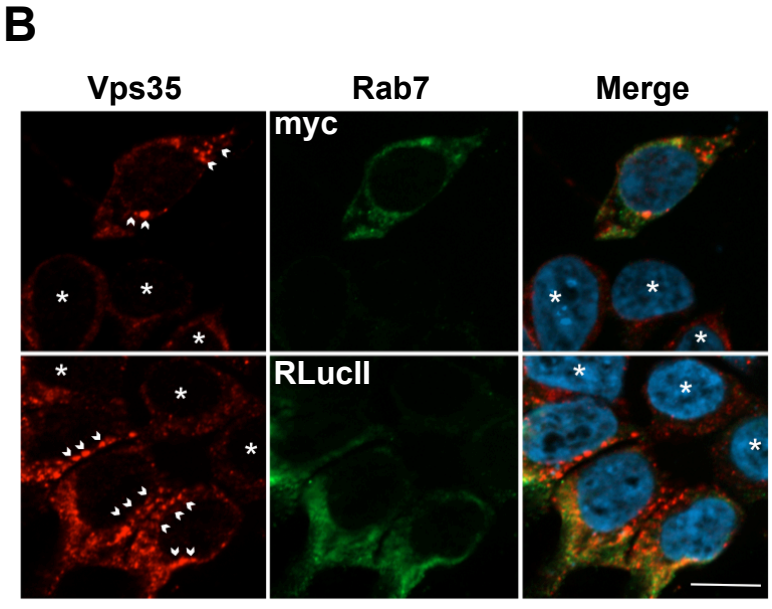

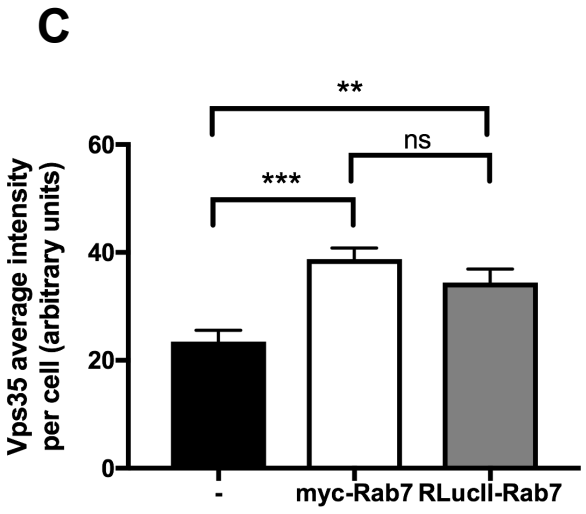

Figure S1. RLucII-Rab7 is properly membrane recruited and functional

(A) HEK-293 or Rab7-KO cells were transfected with myc-Rab7 or RLucII-Rab7. 48 hours post-transfection, a membrane separation assay was performed and samples were subjected to Western blot (Wb) with anti-Vps35, anti-Vps26A, anti-RLucII, anti-myc, anti-Lamp2 antibody (a membrane marker) and anti-α-tubulin (a cytosolic marker). (B) HEK-293 or Rab7-KO cells were transfected with myc-Rab7 or RLucII-Rab7. 48 hours post-transfection, the cells were fixed in 4% paraformaldehyde and immunofluorescence staining was performed with anti-myc (green) or anti-RLucII (green) and anti-Vps26A (red) antibodies. Scale bar = 10 μm. (C) Fluorescence intensity of Vps35 staining was measured in Rab7-KO cells (black bar), Rab7-KO cells expressing myc-Rab7 (white bar) or RLucII-Rab7 (grey bar). Data is represented as mean Vps35 intensity ± SEM from 31, 14, and 16 cells per condition. *** $P < 0.001$, ** $P < 0.01$, ns, not significant, One-way ANOVA with Tukey's post-hoc test.

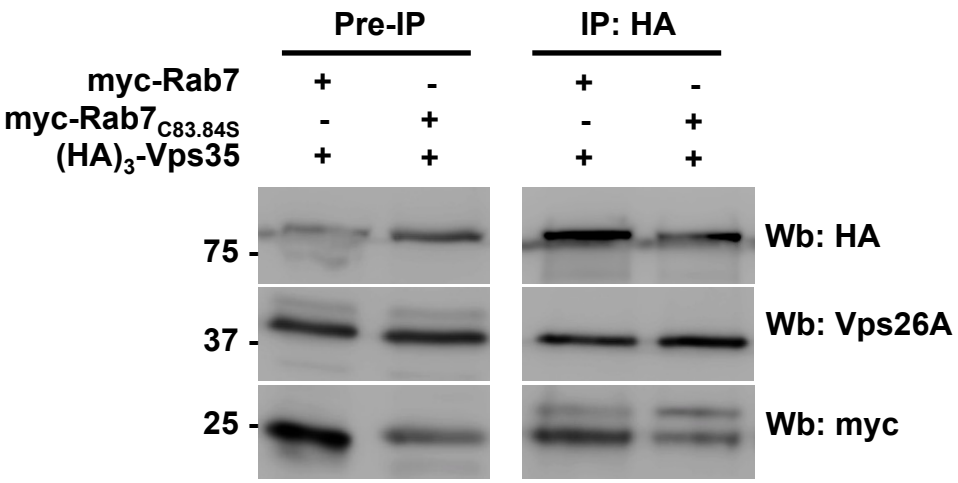

Figure S2. Palmitoylation does not affect the Rab7/retromer interaction *per se*. HEK-293 were transfected with myc-Rab7, myc-Rab7$_{C83,84S}$ or (HA)$_3$-Vps35. 24 hours after transfections, equal amounts of cell lysates from myc-Rab7 or myc-Rab7$_{C83,84S}$ transfected cells were mixed with lysate from HEK-293 expressing (HA)$_3$-Vps35, followed by immunoprecipitation with anti-HA antibody. Eluted samples were loaded onto a 12% polyacrylamide gel and subjected to Western blot (Wb) analysis with anti-myc, anti-Vps26A and anti-HA antibodies.